

SUBCRITICAL TURBULENT TRANSITION IN ROTATING AND CURVED SHEAR FLOWS

Pierre-Yves Longaretti¹, Olivier Dauchot²

¹*LAOG, BP 53X, F-38041, Grenoble, France*

²*GIT/SPEC/DRECAM/DSM CEA Saclay, F-91191, Gif-sur-Yvette, France*

Abstract The effects of global flow rotation and curvature on the subcritical transition to turbulence in shear flows are examined. The relevant time-scales of the problem are identified by a decomposition of the flow into a laminar and a deviation from laminar parts, which is performed for rotating plane Couette and Taylor-Couette flows. The usefulness and relevance of this procedure are discussed at the same time. By comparing the self-sustaining process time-scale to the time-scales previously identified, an interpretation is brought to light for the behavior of the transition Reynolds number with the rotation number and relative gap width in the whole neighborhood (in parameter space) of the non-rotating plane Couette flow covered by the available data.

1. Introduction:

In the last decade or so, a number of breakthroughs have been achieved in the understanding of the onset of turbulence in subcritical shear flows, such as the plane Couette flow and Poiseuille flow, both from an experimental point of view (e.g., Bottin *et al.*, 1998), and a numerical and theoretical one (e.g., Nagata, 1990; Clever and Busse, 1997; Hamilton *et al.*, 1995; Waleffe, 1997; Waleffe, 1998; Waleffe, 2003; Faisst and Eckardt, 2003). In this context, the present contribution has two main objectives: characterize the effects of global flow rotation and curvature in subcritical flows from the available data, and show that these characteristics can be understood at a semi-quantitative level from time-scale considerations. Understanding these questions is essential for geophysical and astrophysical applications, which is one of the motivations of this work. Data on rotating plane Couette flows and Taylor-Couette flows are used in this investigation.

Section 1.2 is devoted to the identification of rotation and curvature characteristic quantities, and relating them to the gross dynamics of the flow. Not

surprisingly, the associated dimensionless numbers reduce to the shear-based Reynolds number, the rotation number, and the relative gap width (for Taylor-Couette flows); the novel point is that the relative gap width is interpreted in terms of a ratio of dynamically relevant time-scales. The experimental data are then reviewed in section 1.3, and the characterization of the available data in terms of the previously defined dimensionless numbers is performed in section 1.4. The last section briefly summarizes the most important results, and discusses their astrophysical implications.

2. The physics of the advection term revisited:

The main objective of this section is to pinpoint the relevant time-scales in globally subcritical, rotating and curved flows, and to relate them to the various contributions of the advection/acceleration term. This turns out to be essential to develop a semi-quantitative understanding of the available data on such flows. In practice, we consider only rotating plane Couette and Taylor-Couette flows. Incompressibility is assumed throughout.

Equations of motions

The relevant time-scales are well-known in rotating plane Couette flows, and follow immediately from the expression of the Navier-Stokes equation in the rotating frame, which reads

$$\frac{\partial \mathbf{u}}{\partial t} + \mathbf{u} \cdot \nabla \mathbf{u} = -\frac{\nabla \pi}{\rho} - 2\boldsymbol{\Omega} \times \mathbf{u} + \nu \Delta \mathbf{u}, \quad (1)$$

with obvious notations (in particular, the centrifugal term has been included in the pressure gradient). They are the shear¹ time-scale $t_s = |S^{-1}|$, the viscous one $t_\nu = d^2/\nu$ (d is the gap in the experiment), and the rotation time-scale related to the Coriolis force $t_\Omega = (2\Omega)^{-1}$ (Ω is the rotation velocity of the flow in an inertial frame), and relate to the advection term, the viscous term, and the Coriolis force, respectively. Correlatively, the flow is described by two dimensionless numbers, the Reynolds number² $Re = t_\nu/t_s = |S|d^2/\nu$, and the rotation number $R_\Omega = \text{sgn}(S)t_s/t_\Omega = 2\Omega/S$.

The situation is less straightforward for Taylor-Couette flows, where the dimensionless number usually associated to the flow geometry, $\eta = r_i/r_o$ (r_i is the inner cylinder radius, r_o the outer one) does not obviously correspond to a ratio of time-scales of the flow. However, on closer inspection, it appears that

¹The convention adopted here is that the sign of S is chosen to be positive when the flow is cyclonic, i.e., when the contributions of shear and rotation to the flow vorticity have the same sign. With the usual choice of axes in plane Couette flows, this implies that $S = -2S_{xy}$, where S_{ij} is the usual deformation tensor.

²This definition differs from the usual one by a factor of 4; this convention is adopted here for consistency with the treatment of Taylor-Couette flows.

this situation arises from a partially incorrect assimilation of the shear time-scale to the advection term. Indeed, in the case of solid body rotation, the shear vanishes, while the advection term does not, due to the global curvature of the flow. One must therefore devise a way to isolate the global shear contribution to the advection term from other contributions.

It turns out that one convenient way to operate such a distinction is to decompose the total flow into its laminar part, and a (not necessarily small) deviation:

$$\mathbf{u} = \mathbf{u}_L + \mathbf{w}. \quad (2)$$

Although the dynamical relevance of the laminar flow to the turbulent one is not a priori obvious, this procedure is suggested and justified by the following considerations:

- Inasmuch as this is feasible, a distinction between global shear, rotation and curvature cannot be operated by a tensorial decomposition of the advection term. For example, it is well-known that both a pure global shear and a global rotation, such as the ones present in rotating plane Couette flows, contribute to the vorticity tensor. In fact, a direct Taylor expansion of the deformation for small displacements shows that one needs to go at least to second order to distinguish the two contributions. Therefore, no tensor constructed from the flow velocity first derivatives will establish the required distinction, by construction.
- The global characteristics of the flow are the same for the laminar and turbulent solutions (geometry, global time-scales, nature of the boundary condition, etc). Therefore, one way to make them appear explicitly in the Navier-Stokes equation is precisely to make the proposed decomposition, as the laminar solution depends everywhere explicitly on these global characteristics. In particular, the laminar and turbulent flows share the same boundary conditions (velocity difference on the boundary, gap width, etc), so that the relative difference between the laminar and turbulent solution is of order unity. This means that the laminar solution is a convenient measure of the turbulent one, although their detailed mechanisms and characteristics are of course essentially different. For example, it turns out that the transition Reynolds number is highly sensitive to various global and/or qualitative characteristics of the laminar flow, such as time-scales, or “distance” in parameter space to the linear stability limits (see section 1.3).

It is useful to point out where this decomposition leads to for the rotating plane Couette flow. This is most naturally done in the rotating frame, so that Eq. (1) becomes

$$\frac{\partial \mathbf{w}}{\partial t} + \mathbf{w} \cdot \nabla \mathbf{w} = S \cdot y \frac{\partial \mathbf{w}}{\partial x} + (2\Omega + S)w_y \mathbf{e}_x - 2\Omega w_x \mathbf{e}_y - \frac{\nabla \delta \pi}{\rho} + \nu \Delta \mathbf{w}, \quad (3)$$

where the pressure gradient balancing the laminar flow Coriolis force has been subtracted out to form the effective generalized pressure $\delta \pi$. Note that on the walls, which specify the global characteristics of the flow, the boundary condition becomes $\mathbf{w} = 0$, quite a featureless constraint: the effect of these boundaries is now explicitly included in the Navier-Stokes equation through the dynamical linear forcing terms on the right-hand side. The real usefulness of this change of point of view comes out when considering Taylor-Couette flows, as we shall now argue.

In this flow, the laminar solution takes the form $\mathbf{u}_L(\mathbf{r}) = r\Omega(r)\mathbf{e}_\theta$. Note that the rotating plane Couette flow can be viewed as a limit of small relative gap width $d/\bar{r} \rightarrow 0$ (\bar{r} is some characteristic radius of the flow), at constant shear, and constant rotation. Then, the effect of the global curvature and rotation will be more easily distinguished from one another if one chooses a formulation of the Navier-Stokes equation which makes the difference with Eq. (3) explicit. To this effect, one must define a characteristic rotation velocity $\bar{\Omega}$, and a characteristic shear³ \bar{S} of the laminar flow. A convenient way to do this is to choose a characteristic radius \bar{r} , and impose $\bar{\Omega} = \Omega(\bar{r})$, $\bar{S} = S(\bar{r})$; the choice of \bar{r} does not need to be further specified for the time being (this point is discussed in the next subsection). Defining $\delta\Omega = \Omega(r) - \bar{\Omega}$ and $\delta S = S(r) - \bar{S}$, the decomposition of the Navier-Stokes equation of the Taylor-Couette flow leads to (r, ϕ, z is the coordinate system in the rotating frame)

$$\begin{aligned} \frac{\partial \mathbf{w}}{\partial t} + \mathbf{w} \cdot \nabla \mathbf{w} = & -\delta\Omega \partial'_\phi \mathbf{w} - (2\bar{\Omega} + \bar{S})w_r \mathbf{e}_\phi + 2\bar{\Omega}w_\phi \mathbf{e}_r - \frac{\nabla \delta \pi}{\rho} + \nu \Delta \mathbf{w} \\ & - (2\delta\Omega + \delta S)w_r \mathbf{e}_\phi + 2\delta\Omega w_\phi \mathbf{e}_r, \end{aligned} \quad (4)$$

where one has used $\partial_\phi \mathbf{w} = \partial'_\phi \mathbf{w} + \delta\Omega w_r \mathbf{e}_\phi + 2\delta\Omega w_\phi \mathbf{e}_r$, with $\partial'_\phi \mathbf{w} \equiv (\partial_\phi w_r)\mathbf{e}_r + (\partial_\phi w_\phi)\mathbf{e}_\phi + (\partial_\phi w_z)\mathbf{e}_z$; this definition is introduced so that the contributions of order $1/\bar{r}$ of the derivatives in the linear terms are separated from the contributions of order $1/d$. This equation is similar⁴ to Eq. (3), except for the last two terms, which consequently are connected to the global flow curvature. Note that, although the definition of $\delta\Omega$ and δS depends on the choice of \bar{r} , the overall variation of these quantities throughout the flow, $\Delta(\delta\Omega)$ and $\Delta(\delta S)$,

³The shear of the laminar flow is defined as $S = rd\Omega/dr = 2S_{r\phi}$ in order to maintain the sign convention adopted for rotating plane Couette flows for cyclonic and anticyclonic rotation.

⁴In the identification of the two equations, note that $r \longleftrightarrow y$ and $\phi \longleftrightarrow -x$. Also, $\delta\Omega \simeq \bar{S}(r - \bar{r})/\bar{r}$, an approximation which holds to $\sim 10\%$ for the range of η explored in the available experiments, a feature needed in the comparison of Eqs. (3) and (4).

does not. In fact, $|\Delta(\delta\Omega)| \sim |\Delta(\delta S)| \sim |\bar{S}|d/\bar{r}$, as can be checked from the laminar flow profile $\Omega(r) = A + B/r^2$. In the process, four time-scales of the incompressible Taylor-Couette flow have been identified: they are the shear time-scale $t_s = |\bar{S}^{-1}|$, the rotation time-scale $t_\Omega = (2\bar{\Omega})^{-1}$, a curvature-related time-scale that one can define as $t_c = |\bar{S}^{-1}|\bar{r}/d$, and, of course, the viscous time-scale $t_\nu = d^2/\nu$. This also shows that the dimensionless geometric number η can be related to the ratio of the shear and curvature time-scales. Taking the limit $d/\bar{r} \rightarrow 0$ ($\eta \rightarrow 1$), one recovers the rotating plane Couette relation Eq. (3).

Characteristic quantities, dimensionless numbers, and the curvature and rotation concepts:

Taylor-Couette flows possess three dimensionless control parameters, which are usually chosen as the Reynolds numbers associated to the inner and outer cylinder rotation velocities, R_i and R_o , and η , the ratio of their two radii. The preceding discussion suggests that one should use instead ratios of time-scales, which have a more direct dynamical meaning. This defines the shear-based Reynolds number⁵ $Re = t_\nu/t_s$, the rotation number $R_\Omega = \text{sgn}(S)t_s/t_\Omega$, and a “curvature” number $R_c = t_s/t_c$. Once a choice of \bar{r} is operated (see below), the procedure is completely specified. This three-dimensional parameter space, in which notable curves and surfaces are drawn, is represented in figure 1.

However, the physical meaning of this procedure is less straightforward than one would like, and this is related to an obvious weakness of Eq. (4): the distinction between the rotation and curvature terms is not absolute when the related time-scales are both dynamically significant. Indeed, any change of definition of $\bar{\Omega}$ and \bar{S} results in a correlative change of $\delta\Omega$ and δS . Nevertheless, the physical meaning is to a large extent unambiguous in at least two different contexts:

- If one changes the rotation velocity of the inner and outer cylinders by the same quantity, this will change $\bar{\Omega}$ by the same amount (independently of the choice of \bar{r}), while leaving all other quantities (\bar{S} , $\delta\Omega$, δS) unchanged. Such changes are obviously an effect of changes in the flow rotation.
- On the other hand, when changes in the flow are operated while maintaining $t_\Omega \lesssim t_c$, the physical meaning of the distinction between the characteristic quantities ($\bar{\Omega}$, \bar{S}) and the deviations from these ($\delta\Omega$, δS)

⁵We use the same Reynolds number definition for rotating plane Couette and Taylor-Couette flows, based on the total gap width and total velocity difference. Consequently, the quoted Reynolds numbers for plane Couette flows differ from the ones in the literature by a factor of 4.

is blurred. This is the case in particular when the cylinders are counter-rotating, or when one cylinder is at rest, for *any* choice of \bar{r} . In such a context, changes in both parameters (the rotation number and the curvature number) describe the effect of a change in the flow curvature, as they are both proportional to d/\bar{r} , and vanish if the limit of vanishing global curvature is taken while enforcing the $t_\Omega \lesssim t_C$ relation.

This clearly shows that rotation and curvature are not interchangeable concepts, although they have a non-negligible overlap. In this context, the denominations “rotation number” and “curvature number” are somewhat conventional and partially misleading, even if justified to some extent by the preceding considerations. In the (R_Ω, R_C) plane, changes along lines of constant R_C correspond to changes of rotation, but there are infinitely many paths involving changes of both parameters and corresponding to changes of curvature from a physical point of view. Furthermore, most paths do not lead to any clear-cut distinction between curvature and rotation changes in the flow. Of course, once a reference curvature path is chosen (e.g., the path with the inner cylinder at rest, corresponding to the inviscid linear stability limit on the cyclonic side, shown as curve (4) on figure 1), every point in the (R_Ω, R_C) plane can be connected to the non-rotating plane Couette flow (the origin in the plane), first through a change of curvature along the chosen curvature path until the desired curvature number is reached, and then through a change of rotation at constant R_C . However, this distinction is only relative.

Obviously, this situation is intrinsic, as one cannot curve a straight flow, without at the same time making it rotate. The procedure outlined here nevertheless leads to the definition of well-defined parameters, which have a dynamical interpretation. It is their physical meaning in terms of rotation and curvature which is partially ambiguous. Furthermore, these parameters turn out to be useful to understand basic features in the data on the subcritical transition to turbulence, as discussed in the next section.

The remaining point to be addressed relates to the choice of \bar{r} . The preceding discussion makes it clear that this choice is not unique. The definition we have adopted here is $\bar{r} \equiv (r_i r_o)^{1/2}$, as suggested in Dubrulle *et al.*, 2004 (r_i and r_o are the inner and outer radius, respectively). This choice is partially motivated by the compactness of the resulting expressions for the dimensionless numbers introduced above:

$$Re = \frac{2\bar{r}}{r_o + r_i} \frac{\bar{r}|\Omega_o - \Omega_i|d}{\nu} = \frac{2}{1 + \eta} |\eta R_o - R_i|, \quad (5)$$

$$R_\Omega = \frac{r_i \Omega_i + r_o \Omega_o}{r_o r_i} \frac{d}{\Omega_o - \Omega_i} = (1 - \eta) \frac{R_i + R_o}{\eta R_o - R_i}, \quad (6)$$

$$R_C = \frac{d}{\bar{r}} = \frac{1 - \eta}{\eta^{1/2}}. \quad (7)$$

Note that, for the range of values of η explored in the available experiment, $Re \simeq \bar{r}|\Delta\Omega|d/\nu$, and $R_\Omega \simeq (2\bar{\Omega}/\bar{r})(d/\Delta\Omega)$ (within a few percents).

3. Subcritical transition in rotating plane Couette and Taylor-Couette flows:

Considering a laminar flow of given dimensionless numbers (rotation, curvature, and Reynolds), two different things can happen when increasing the Reynolds number: either the flow will undergo a linear instability first (supercritical transition), or it will undergo a laminar-turbulent transition first (globally subcritical transition). The second option may happen whether the flow is linearly unstable or not.

The Reynolds number characterizing subcritical transition in a system is not a quantity that can be measured with absolute precision, as it depends to some extent on the experimental protocol used in its determination. For example, the laminar-turbulent transition Reynolds number is generically larger than the turbulent-laminar one. Furthermore, the flow is intermittent over a range of Reynolds numbers in the vicinity of this transition. This leads to some differences in the determined Reynolds transition values, even when the same data are used by different authors; however, the dispersion of the data in a given author's choice is much smaller. Overall, the resulting range of values (at given dimensionless numbers) is uncertain within less than a factor of ~ 2 ; we shall ignore this problem here, as we are only interested in characterizing qualitative trends and orders of magnitude.

With this convention, both supercritical ($Re = R_c$) and globally subcritical ($Re = R_g$) transitions are characterized by surfaces in the three dimensional space (R_Ω, R_C, Re). Only particular lines on these surfaces have been probed by the available experiments. Obviously, the supercritical and subcritical surfaces meet somewhere in this space, so that one needs to characterize both surfaces.

It turns out, from a practical point of view, that the supercritical surface (manifold (1) in figure 1) is sufficiently well captured by the analytic approximation derived by Esser and Grossmann, 1996, for Taylor-Couette flows, although it relates only to axisymmetric perturbations (in other words, the non-axisymmetric perturbations seem to play little role in the definition of the supercritical transition). The rotating plane Couette flow is included in the limit $\eta \rightarrow 1$. For the relatively high Reynolds numbers of interest for subcritical transitions to turbulence (> 1000), the dependence of the supercritical surface on the Reynolds number is very steep, and the surface is well-approximated by the inviscid linear stability limit (curves (2) of figure 1). This explains that

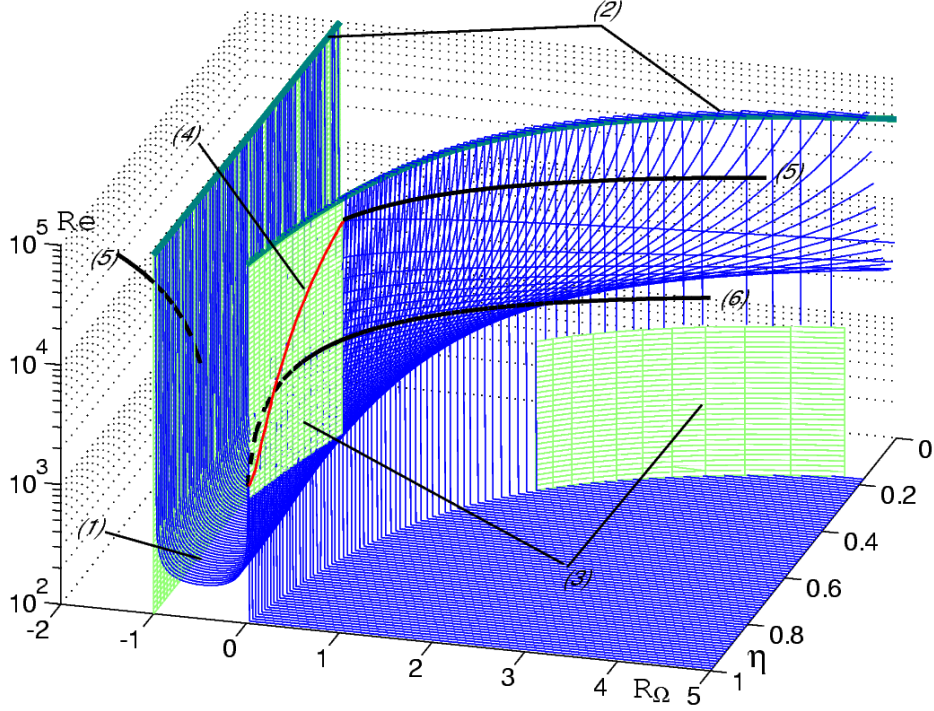


Figure 1. Stability boundaries in the (Re, R_Ω, R_C) parameter space (η is used as a measure of R_C on this graph). Manifold (1): linear stability threshold. Dark curves (2): linear stability threshold in the inviscid limit. Manifold (3): extrapolation of the inviscid criteria throughout the full Reynolds space (partially shown for readability). Curve (4): globally subcritical threshold obtained with inner cylinder at rest (see text). Other curves: globally subcritical thresholds obtained at fixed value of η [(5): $\eta = 0.7$; (6): $\eta = 1$] (see text).

the limit of the subcritical regime in the (R_Ω, R_C) plane is well-approximated by the inviscid limit. Linear instability follows somewhere in the fluid in this limit if

$$-1 \leq \frac{2\Omega(r)}{S(r)} \leq 0, \quad (8)$$

at this location (this is equivalent to the constraint put by the Rayleigh discriminant). Asking that the fluid is everywhere stable with respect to this criterion translates into $R_\Omega < -1$, or $R_\Omega > (1 - \eta)/\eta$.

The data on subcritical transition discussed here are those of Wendt (1933), Taylor (1936), Tillmark and Alfredsson (1996), and Richard (2001); they are represented on figure 2. One could also include data on counter-rotating cylinders (Andereck, Liu and Swinney, 1986; Prigent *et al.*, 2003), but these occupy

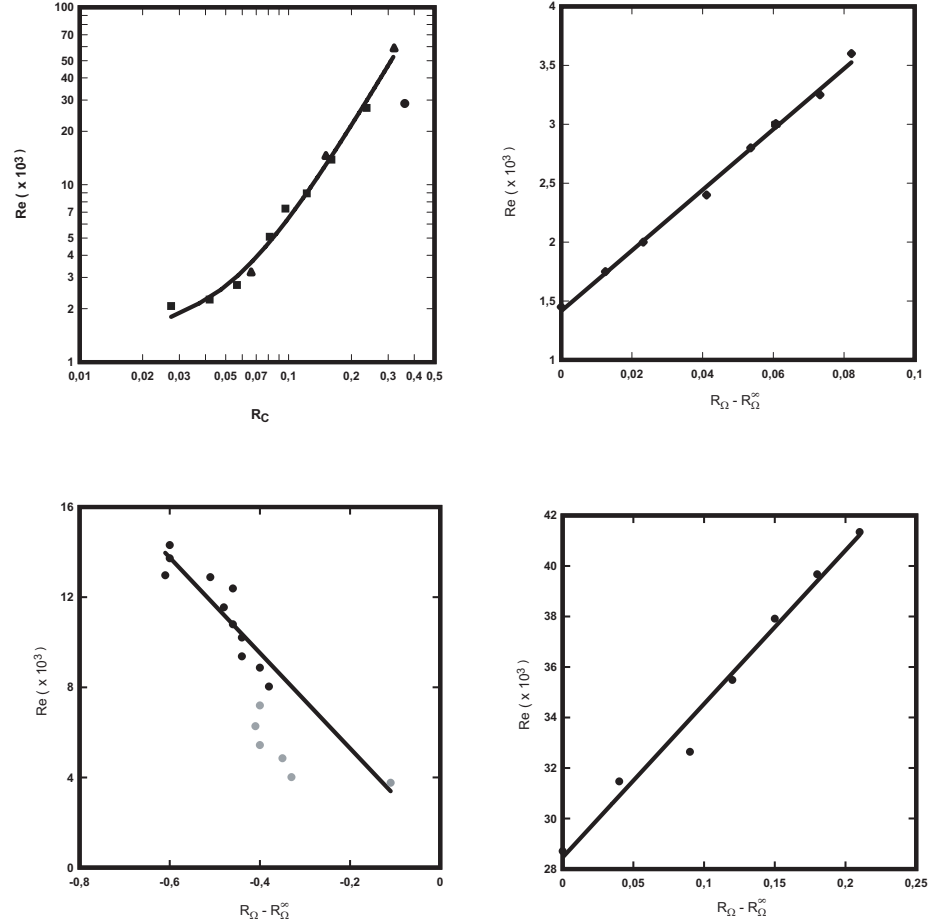


Figure 2. Data on subcritical transition. Upper left: data of Wendt (1933) and Taylor (1936), for cyclonic rotation, with the inner cylinder at rest, for varying η ; this shows the dependence on the curvature number in cyclonic flows. Upper right: data of Tillmark and Alfredsson (1996) for rotating plane Couette flows ($\eta = 1$). Lower left and lower right: data of Richard (2001), for anticyclonic and cyclonic rotation, respectively ($\eta = 0.7$). On the last three graphs, the curvature number is held fixed, so that the data show the dependence of the transition Reynolds number on the rotation number. The solid lines represent best quadratic or linear fits to the data. $R_\Omega^\infty = (1 - \eta)/\eta$ for cyclonic flows, and $R_\Omega^\infty = -1$ for anticyclonic ones.

only a small area in the (R_Ω, R_C) plane, and bring little constraint on the trend of the transition Reynolds number with the rotation and curvature numbers (see Longaretti and Dauchot, 2004 for a discussion of counter-rotating data).

The data are well parameterized by the following approximate formula (the + and - sign refer to cyclonic and anticyclonic flows, respectively)

$$R_g^\pm(R_\Omega, R_C) = R_{PC}^\pm + a^\pm(\eta)|R_\Omega - R_\Omega^{\infty,\pm}| + b^\pm R_C^2, \quad (9)$$

with $R_{PC}^+ \simeq 1400$, $R_{PC}^- \simeq 1100 \sim R_{PC}^+$, $21000 \lesssim a^\pm \lesssim 61000$, $2 \times 10^5 \lesssim b^+ \lesssim 6 \times 10^5$, $b^- \ll b^+$, and where $R_\Omega^{\infty,+} = (1 - \eta)/\eta$, and $R_\Omega^{\infty,-} = -1$. This is discussed in detail in Longaretti and Dauchot, 2004, and Dubrulle *et al.*, 2004.

The most notable characteristics of this dependence are the following:

- The linear dependence on the rotation number, and quadratic one on the curvature number.
- The rather steep dependence with both numbers (a^\pm and b^+ are large numbers).
- The apparent symmetry between cyclonic and anticyclonic rotation number dependence, and the absence of dependence on the curvature on the anticyclonic side ($b^- \simeq 0$).

The next section discusses these features; in particular, the strength of this dependence is explained in order of magnitude on the basis of time-scale considerations.

4. Data interpretation:

The linear and quadratic dependence just pointed out can be viewed as the result of a Taylor expansion. For cyclonic rotation, this expansion is performed around the non-rotating plane Couette flow, first in terms of R_C along curve (4) on figure 1, and then away from it, at constant R_C , in terms of R_Ω . For anticyclonic rotation, the expansion depends only on R_Ω , at least for $\eta > 0.7$, and is performed from the marginal stability state, at $R_\Omega \simeq -1$.

Linear dependence

The linear dependence with R_Ω is neater on the cyclonic data than on the anticyclonic one, but the data extend less far on the cyclonic side, unfortunately. The increased dispersion on the anticyclonic side has several reasons:

- Both cylinders need to be rotating at much higher speed than on the cyclonic side to reach the subcritical turbulent transition. This automatically reduces the precision of the measurements.
- The quantity R_Ω amplifies the uncertainty due to small errors in the determination of the cylinder angular velocities at transition.
- There is an important intrinsic difference between the cyclonic and anticyclonic marginal stability limits. On the cyclonic side, instability begins at a single location (the inner radius), whereas on the anticyclonic

side, marginal stability applies throughout the fluid (this follows because the constant angular momentum solution is a laminar solution of the Taylor-Couette flow). Equivalently $2\delta\Omega(r) + \delta S(r) = 0$ at the anticyclonic marginal stability limit. Therefore, the fluid is much more sensitive to a potential linear instability. In particular, the unavoidable Eckmann circulation can much more easily make the criterion Eq. (8) satisfied somewhere in the flow on the anticyclonic side than on the cyclonic one. We believe that this feature most likely explains why Richard's data show only a weak dependence of the transition Reynolds number on the rotation number out to $|1 + R_\Omega| \simeq 0.35$, and then a sharp increase to reach back the linearly varying regime. The related data points are shown as thin dots in the lower left quadrant of Fig. 2, and not used in the linear fit.

Note that the mutual cancellation of a part of the curvature terms in Eq. (4) at the anticyclonic marginal linear stability limit just pointed out also provides a natural explanation for the apparent absence of dependence of the anticyclonic data on the curvature number.

Quadratic dependence

The quadratic dependence of the data on the gap width when keeping the inner cylinder at rest has already been pointed out by Zeldovich, 1981, and Richard and Zahn, 1999. At least three explanations of this behavior have been put forward in the literature (Zeldovich, 1981; Dubrulle, 1993; Longaretti, 2002). These will be commented below.

Let us first note that, in plane Couette flows, transition occurs at a constant Reynolds number $Re = \bar{S}d^2/\nu$. Therefore, at a given shear \bar{S} , the scale d is the characteristic scale of turbulence in such a system. Conversely, in the quadratic asymptotic regime, $[Re \propto (d/\bar{r})^2]$, transition occurs at constant $Re^* = \bar{S}\bar{r}^2/\nu$ ($= b^+$), a point already made by Richard and Zahn, 1999. Consequently, the characteristic radius \bar{r} instead of the gap d characterizes the transition at a given shear. This unambiguously points out curvature and not rotation as the source of this behavior, consistently with the discussion of section 2.

Dubrulle, 1993, explains the quadratic behavior by considering the growth of finite amplitude local defects in the laminar profile. However, only WKB modes of instability created by the defects are considered, for which the scale \bar{r} cannot play any role. This is why we believe that this analysis cannot capture the transition mechanism.

Zeldovich, 1981, phenomenological explanation is based on the following two ideas:

- The transition Reynolds number may depend on the single time-scale ratio $Ty(r) = 4\kappa^2(r)/S^2(r)$ at some appropriately chosen radius in the

flow: $R_g = f(Ty)$; $\kappa(r) = [2\Omega(2\Omega + S)]^{1/2}$ is the epicyclic frequency, i.e., the frequency of oscillation of the whole fluid, under the combined action of the shear and the Coriolis force.

- A “split-regime” of instability may occur, in which the inner portion of the flow undergoes a transition to turbulence at lower Reynolds number than the whole flow, once a large enough relative gap width is reached.

Considering the relative ambiguity in the distinction between the rotation and curvature time-scale discussed in section 1.2, one may indeed ask whether a single time-scale would be sufficient to understand the data. This would imply that Taylor-Couette flows possess a hidden redundancy, and could be described by two appropriately chosen parameters, and not three. However, the extended set of data used here does not support this idea, although a larger body of experimental results is probably needed to ascertain this result.

Longaretti, 2002 has developed an alternate phenomenology of subcritical shear flow turbulence. It relies on the one hand on a turbulent viscosity description, in which the characteristic length is identified to the top of the Kolmogorov cascade; on the other hand it makes use of the constraint that a subcritical shear flow is out of thermodynamic equilibrium and tries to restore equilibrium by transporting momentum across the shear, and, to do so, chooses the most efficient of the two means at its disposal (laminar or turbulent transport). This provides scaling laws for the characteristic length and velocity of turbulent eddies, by relating them to the Reynolds number of transition to turbulence. By further noting that for large enough gap widths, the turbulent eddies must unavoidably scale with the radius and not the gap, the quadratic regime is recovered.

Orders of magnitude

The last point we wish to address is the origin of the large values the coefficients a and b which appear in the characterization of the data performed in Eq. (9). We mostly consider cyclonic flows, for which the physics is best understood

As mentioned in the introduction, an important breakthrough in the understanding of subcritical turbulence in non-rotating plane Couette flow comes from the work of Waleffe, 1997, who analyzed by the means of quasi-linear theory a turbulent self-regeneration process previously observed in the numerical simulations of Hamilton *et al.*, 1995. These last authors have tracked down turbulence to the smallest unit where it is self-sustained by reducing appropriately the simulation box size and the Reynolds number. A very important feature of the identified self-sustaining process is that it has a rather long time-scale compared to the shear:

$$t_{ssp}^+ \sim 100\bar{S}^{-1}. \quad (10)$$

and that the scales involved in the self-regeneration mechanism are comparable to the flow width. This time-scale is the shortest of all the mechanisms found in the systematic reduction of the flow, and thus corresponds to the most robust one, which involves two streamwise rolls in the spanwise direction. These streamwise rolls, first observed by Dauchot and Daviaud, 1995, typically scale on the gap width. Accordingly, it is very likely that such a long time-scale is a generic feature in non rotating plane Couette flows, because of the large ($Re_{PC}^+ \sim 1500$) Reynolds number of transition to turbulence which are always observed in these systems. Such a large Reynolds number constrains the viscous diffusion time at the scales involved in the self-regeneration mechanism. Typically for a length-scale $d/4$, the equality of the viscous time $t_\nu = (d/4)^2/\nu$ with t_{ssp}^+ would indeed leads to $Re_g = 1600$. Such a scale ($d/4$) is characteristic of the thickness of the streaks, apparently the smallest characteristic scale of the process.

From a physical point of view, one expects that the contributions of either rotation or curvature become comparable to Re_{PC}^+ in Eq. (9) when the rotation or curvature time-scales decrease to become comparable to t_{ssp}^+ . Correlatively, the fact that this happens when the rotation and curvature numbers are $\simeq 1/20$ comes as no coincidence. Indeed, the timescale associated with the Coriolis term is $t_\Omega \simeq (2\bar{\Omega})^{-1}$, while the timescale associated with the curvature terms is $t_C \simeq (\delta\Omega)^{-1} \sim \bar{S}\bar{r}/d$. They become comparable to t_{ssp}^+ as defined in Eq. (10) when R_Ω or R_C exceeds 10^{-2} , which is remarkably close to the actual value of $1/20$, considering the qualitative nature of the argument. This physical constraint is also what primarily determines the magnitude of a^+ and b^+ (once the form of the dependence on R_Ω and R_C is known). Indeed, in rotating plane Couette flows, requiring $a^+ R_\Omega \gtrsim Re_{PC}^+$ when $R_\Omega \gtrsim 1/20$, implies that $a^+ \sim 10^4$. Similarly, in Taylor-Couette flows, requiring that $b^+ R_C^2 \gtrsim Re_{PC}^+$ when $R_C \gtrsim 1/20$ leads to $b^+ \sim 10^5$.

One can see that the rather large values of the transition Reynolds number, as well as of the coefficients characterizing the effect of rotation (a^+) and curvature (b^+) can be ascribed to a single origin: the rather large ratio of the turbulence self-regeneration process to the shear time scale. Still, we do *not* infer that the self-sustaining mechanism proposed by Waleffe is valid in the presence of rotation. We just use the fact that in order to modify or even suppress this mechanism, the rotation or curvature effects must have timescales of the same order. On the contrary, the above analysis clearly indicates that a better understanding of this process in the framework of curved shear flows, and identifying it in the presence of rotation, is of primary importance for future progress.

The self-sustaining process has not yet been identified at the anticyclonic marginal stability limit, and its nature is not known. However, one can reverse the reasoning expressed right above to reach the conclusion that its characteristic time-scale is also $\sim 100\bar{S}^{-1}$. Testing this conjecture would bring support to the framework developed here to analyze and understand the data.

5. Conclusions and implications:

We feel that this work brings to light a few important points, which we believe to be of potentially more general applicability than what was done here:

- It is both meaningful and useful to decompose the Navier-Stokes equation into a laminar part of the flow, and a deviation from the laminar flow. This helps identifying the relevant time-scales in the flow, and isolating which “portion” of the advection term is directly related to the physics described by the Reynolds number. The same procedure is also useful to relate various flows to one another.
- The general trends and features of the transition Reynolds number data can be understood with the help of the previously identified time-scales, and over a reasonably extended fraction of the parameter space, once the turbulence self-sustaining process time-scale is identified at one point in the parameter space. The procedure in turns constrains to some extent the time-scale of the self-sustaining process in the domain where data are available, a point we have only briefly touched upon in the preceding section.

In the process, we have tried to elucidate a little more the relation between the flow global rotation and its global curvature. We found that rotation and curvature effects most probably cannot be accounted for by a single time-scale, as suggested by Zeldovich, 1981, but that two time-scales are required, in accordance with the fact that Taylor-Couette flows are characterized by two dimensionless numbers besides the Reynolds number.

The data described here, and the analysis we have developed, have some bearing to a related astrophysical problem, namely, the existence of subcritical turbulence in keplerian accretion disks, a question which has been the object of an important debate in the astrophysical community over the three or four past decades. Such disks are observed in relation to the formation of young stars; they are also believed to be present in a variety of other astrophysical objects, such as active galactic nuclei, microquasars, and so on. A large scale keplerian profile ($\Omega(r) \propto r^{-3/2}$) follows if the disk is cold enough. The profile can nevertheless stochastically deviate from keplerian on scales comparable to the disk scale height $h \ll r$. Young (proto-)star disks are also probably not

ionized enough for MHD processes to be relevant over a significant fraction of their extent.

The microscopic transport in these disks is known to be many orders of magnitude smaller than the one inferred from the observations, so that these disks are believed to be turbulent. Hydrodynamic Keplerian disks are linearly stable in their most simple flavors. It was believed until the mid-90's that they were nevertheless hydrodynamically turbulent, on the basis of the experimental evidence of subcritical turbulence in non-rotating Couette flows.

This belief was challenged by the numerical simulations of Balbus *et al.*, 1996, and Hawley *et al.*, 1999. These authors have studied whether keplerian disks are locally turbulent, by reducing the Navier-Stokes equation in the disk to Eq. (3), with “shearing-sheet” boundary conditions (they ignore the disk vertical stratification), thus asking the question in a framework which is extremely close to the one studied here. They found that a dynamically significant and stabilizing Coriolis force prevents the appearance of turbulence for keplerian-like flows ($R_\Omega = -4/3$), up to to the highest resolution achieved in the simulation (256^3 with finite-difference codes; see the referenced papers for detail).

These simulations have had a very large impact in the astrophysics community, where the now most largely spread opinion is that a linear instability is needed for turbulence to show up, a somewhat excessive position. However, the experimental results of Richard, 2001, seem to imply that keplerian-like flows should be turbulent at very modest (in astrophysical standards) Reynolds numbers. The problem is currently reinvestigated from a numerical point of view (Lesur and Longaretti, *in preparation*). Preliminary results indicate that the Coriolis force does not prevent the existence of turbulence in rotating plane Couette flows, but of course alters the turbulence properties, as one would expect. However, the relevance of subcritical hydrodynamic turbulence to accretion disk transport remains to be more precisely investigated.

References

- Andereck, C.D., Liu, C.C., and Swinney, H.L. (1986). Flow regimes in a circular Couette system with independently rotating cylinders. *J. Fluid Mech.*, 164: 155-183.
- Balbus, S.A., Hawley, J.F., and Stone, J.M. (1996). Nonlinear stability, hydrodynamical turbulence, and transport in disks, *Astrophys. J.*, 467: 76-86.
- Bottin, S., Dauchot, O., Daviaud, F., and Manneville P. (1998). Experimental evidence of stream-wise vortices as finite amplitude solutions in transitional plane Couette flow. *Phys. Fluids*, 10, Issue 10: 2597-2607.
- Clever, R.M., and Busse, F.H. (1997). Tertiary and quaternary solutions for plane Couette flow. *J. Fluid Mech.*, 344: 137-153.
- Dauchot, O., and Daviaud, F. (1995). Finite amplitude perturbation and spot growth mechanism in plane Couette flow, *Phys. of Fluids* 7: 335-343.

- Dubrulle, B. (1993). Differential rotation as a source of angular momentum transfer in the Solar Nebula, *Icarus*, 106: 59-76.
- Dubrulle, B., Dauchot, O., Daviaud, F., Longaretti, P.-Y., Richard, D., and Zahn, J.-P. Stability and turbulent transport in rotating shear flows: prescription from analysis of cylindrical and plane Couette flow data. *Submitted to Phys. of Fluids*.
- Esser, A., and Grossmann, S. (1996). Analytic expression for Taylor-Couette stability boundary, *Phys. Fluids*, 8: 1814-1819.
- Faisst, H., and Eckardt, B. (2003). Travelling waves in pipe flow. *Phys. Rev. Lett.*, 91: 224502.
- Hamilton, J.H., Kim, J., and Waleffe, F. (1995). Regeneration mechanisms of near-wall turbulence structures. *J. Fluid Mech.*, 287: 317-348.
- Hawley, J.F., Balbus, S.A., and Winters, W.F. (1999). Local hydrodynamic stability of accretion disks, *Astrophys. J.*, 518: 394-404.
- Longaretti, P.-Y. (2002). On the phenomenology of hydrodynamic shear turbulence, *Astrophys. J.*, **576**, 587-598.
- Longaretti, P.-Y., and Dauchot, O. Global rotation-curvature time-scales, and the subcritical transition to turbulence in shear flows. *Submitted to Phys. of Fluids*.
- Nagata, M. (1990). Three-dimensional finite-amplitude solutions in plane Couette flow: bifurcation from infinity. *J. Fluid Mech.*, 217: 519-527.
- Prigent, A., Grégoire, G., Chaté, H., and Dauchot, O. (2003). Long wavelength modulation of turbulent shear flows. *Physica D*, 174: 100-113.
- Richard, D. (2001). *Instabilités hydrodynamiques dans les écoulements en rotation différentielle*. PhD thesis. Université de Paris VII.
- Richard, D., and Zahn, J.-P. (1999). Turbulence in differentially rotating flows, *Astron. Astrophys.*, 347: 734-738.
- Taylor, G.I. (1936) Fluid friction between rotating cylinders, *Proc. Roy. Soc. London*, A 157: 546-564.
- Tillmark, N., and Alfredsson, P.H. (1996). Experiments on rotating plane Couette flow. In *Advances in Turbulence VI*. (eds, Gavrilakis *et al.*), p. 391-394; Kluwer.
- Waleffe, F. (1997). On a self-sustaining process in shear flows. *Phys. Fluids*, 9: 883-900.
- Waleffe, F. (1998). Three-dimensional coherent states in plane shear flows. *Phys. Rev. Lett.*, 81:4140-4143.
- Waleffe, F. (2003). Homotopy of exact coherent structures in plane shear flows. *Phys. Fluids*, 15: 1517-1534.
- Wendt, G. (1993). Turbulente Strömung Zwischen Zwei Rotierenden Konaxialen Zylindern, *Ing. Arch.*, 4: 577-595.
- Zeldovich, Y.B. (1981). On the friction of fluids between rotating cylinders, *Proc. Roy. Soc. London A*, 374: 299-312.